Comparison of gamma calibration methods for fringe projection profilometry

Jorge A. Contreras[1], Jorge L. Flores[1], and Sotero Ordones[2]

[1] Electro-Photonics Engineering Department, University of Guadalajara, Av. Revolución 1500, Guadalajara, Jalisco, Mexico
[2] Shanghai Institute of Optics and Fine Mechanics, Chinese Academy of Sciences, Shanghai 201800, PR China

Abstract. A fringe projection profilometer is a system that retrieves tridimensional surface information by digital signal processing of sinusoidal patterns, projects and captures these patterns as they are being spatially modulated by an object. In this paper, we address the problem of calibrating the nonlinear intensity response of the projector, namely gamma distortion, by proposing a new calibration method that requires only a sinusoidal pattern to estimate the gamma factor. This value is used to generate and project the new set of fringe patterns for which we perform the inverse gamma compensation. We also compare the performance of the proposed method with the polynomial method and the least squares method. The numerical accuracy of these three models was compared by computer simulations, and we subsequently analyzed their performance in mitigating gamma distortion in experimental data. The results show the effectiveness of the proposed method in estimating and correcting gamma distortion.

Keywords: Fringe projection profilometry, Nonlinear intensity response, Calibration.

1 Introduction

Three-dimensional measurement theory based on structured light has developed rapidly with the rapid development of computer technology, optical and optoelectronic devices. Systems are already in place that allow us to achieve this contact system like the coordinate measuring machines (CMMs), time of flight (ToF) cameras, stereo vision sensors, and structured light projection systems. The most important in the industry is the CMM because of its high accuracy and not being sensitive to the reflectiveness of the object, it gets done through measurement of coordinates of an object in a point-to-point contact although it's not very efficient [1].

In contrast with the CMM, the fringe projection profilometer (FPP) is one of the most efficient systems, so much so that even real-time measurements are being actively considered and worked on [2]. The FPP is an instrument that utilizes structured light patterns to measure tridimensional object surfaces, and has several applications: in medical fields, automotive industry, reverse engineering, archaeological preservation, among others [3].

https://doi.org/10.61728/AE20255114

The 3D fringe pattern profilometer is composed of a camera and a projector. The latter projects sinusoidal patterns on a surface to be measured, where those undergo a spatial modulation, which is captured. Subsequently, the tridimensional surface is extracted from the acquired patterns through a phase shift algorithm and a phase unwrapping one [4, 5, 6]. Despise its simplicity of construction, each element componing the system introduces a set of distortions to the captured patterns [7,8], those distortions compromise system reliability, reducing the precision and accuracy of the measurements made. Regardless of the progress made, there is still room for improvement, so we propose a method for calibration of the nonlinear intensity response of a video projector and compared its performance with 2 other literature methods.

We start discussing the basic theory of phase retrieval in fringe projection. Second, we discuss the nonlinearity of the projector and how to correct according to the power law. Next, we talk about 2 literature methods, the first linearizing the projector intensity response estimating a high-degree polynomial on a ramp function projected in a reference plane [9]. The second estimates a global gamma constant by adjusting the least-squares plane to the estimated phase coming from the reference plane [10], and the proposed one that estimates by adjusting a gamma induced ideal signal to the captured pattern. In the simulation method we make a comparison using numerical simulations to understand the performance of each model as a function of the noise level and its respective processing time.

In the work, we present a new approach to estimate the gamma of a projection system used for reconstructing and measuring 3D surfaces. The estimation is performed as an optimization problem. Also, we compare our proposal with the methods that have been reported in the literature.

The remainder of this paper is structured as follows: Section 2 describes the proposed theory of each method for gamma correction. Section 3 presents experimental results and comparative analysis based on numerical simulations. Finally, Section 4 presents the conclusion of the presented work.

2 Theorical framework

2.1 Fringe pattern profilometer (FPP)

A basic structured light projection system is illustrated in Fig 1. The setup consists of a computer to generate and process fringe patterns, a digital light projector to project the generated patterns, a high-resolution camera (CCD, Charged coupled device) that is used to acquire the fringe patterns modulated by the object surface under test, and the reference plane used to calibrate the system. Where ψ is the angle between the camera and the projector, h is the height of the object, and p is the fringe pattern pitch.

In general, to measure a tridimensional surface by the projection of sinusoidal intensity patterns, one project and acquire sequence patterns shifted by the known phase angles. The acquired patterns can be described as:

$$\mathrm{I}_n(x,y) = I_0(x,y) + I_{mod}(x,y) \cdot cos(\varphi(x,y) + \delta_n),\ (n = 1,2,3,\dots,N)\ , (1)$$

here $(x, y) \in R^2$ is the pixel location; $I_0(x, y)$, and $I_{mod}(x, y)$ are the background and intensity modulation, respectively. While $\varphi(x, y)$ is the phase to be retrieved containing the encoded information of the three-dimensional surface of the object, and δ_n is a known phase shift defined as $2\pi n/N$, where N is the number of phase steps or patterns to be projected.

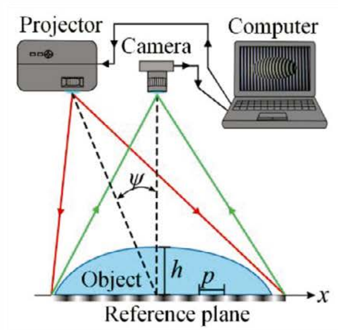

Fig. 1. Setup sketch of fringe projection profilometer.

Once the patterns are acquired, the phase can be estimated by phase shift algorithms, e.g., the phase $\varphi(x, y)$ can be solved by [5]

$$\varphi_w(x, y) = \tan^{-1}\left[\frac{\sum_{n=1}^{N} I_n(x,y)\sin(\delta_n)}{\sum_{n=1}^{N} I_n(x,y)\cos(\delta_n)}\right], \ \delta_n = \frac{2\pi n}{N}. \quad (2)$$

This expression provides the wrapped phase $\varphi_{w(x,y)}$ ranging $\in (-\pi, \pi]$. δ_n is the phase shift that that are equidistant angles in a range of $[0, 2\pi)$. The wrapped phase is later processed through an unwrapping phase algorithm that converts the phase defined in a range $(-\pi, \pi]$ in a continuous range. As a final step, we convert the retrieved phase to height though phase-height calibration procedure [12].

2.2 Gamma correction

A variety of devices used for image projection, capture, printing, and displaying response according to the power law, i.e.

$$I_{out} = I_{in}{}^{\gamma}, \quad (3)$$

where, γ is a positive constant (By convention, the exponent in the power-law equation is referred to as gamma). According to Fig. 1 and the acquired patterns I_{out} will be distorted by this nonlinear transformation, assuming that one generated ideal sinusoidal intensity patterns, when the gamma value is different from 1.

By inspection of the Eq. (3), one could correct the distortion in the acquired patterns, if we know the gamma value, before projecting patterns, i.e.,

$$I_{in} = (I_{out})^{1/\gamma} = (I_{in}{}^{\gamma})^{1/\gamma}. \quad (4)$$

Although this relation gives us an easy way to correct the gamma. In real systems, one required to estimate the gamma value and digitally generate sinusoidal intensity patterns power to $1/\gamma$. In Fig 2, we can see how the intensity response of the projector modified the gray levels to be projected and how it distorts the acquired fringe patterns. For example, in systems based on the projection of sinusoidal intensity patterns the nonlinear response introduces higher order harmonics, which introduced phase errors when fringe patterns are demodulated by phase shifting algorithms.

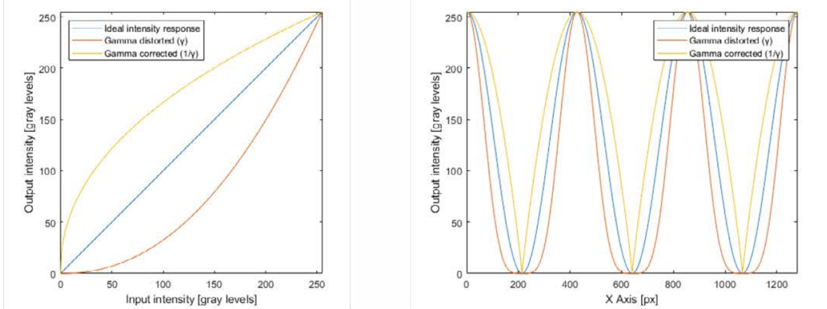

(a) (b)

Fig. 2. (a) Plots of Eq. (3) and Eq. (4) for: blue line, γ equal to 1 and for yellow and red lines equal to 2.2. (b) Linear response of the digital light project when the input is a sinusoidal intensity and gamma values according with cases shown in (a)

3 Calibration mathematical models

3.1 Preprocessing image

In addition to the gamma problem, the reflectance of the object and illuminance is not uniform on the object's surface. Thus, the Eq. (4) should be rewritten as

$$I_a(x,y) = F(x,y)I_p(x,y) + \eta(x,y). \tag{5}$$

Where $I_a(x,y)$ is the acquired intensity pattern under more realistic conditions, $I_p(x,y)$ is the input pattern, $\eta(x,y)$ is noise, and $F(x,y)$ is reflectance and emittance of the projector. As we can see in equation (5), to get an ideal projected pattern, we need to remove the inhomogeneities in the acquired patterns that are due reflectance and no uniform illumination projector. One way to estimate the $F(x,y)$ is projecting a pattern with constant illuminance on the reference plane, as shown in Fig. 3(a) and perform basic digital manipulations between images, e.g.

$$\frac{I_a(x,y)}{I_C} = \frac{I_d(x,y)F(x,y)+\eta(x,y)}{I_C}, \tag{6}$$

where $I_d(x,y)$ is the constant illuminance pattern and I_C is the known constant illuminance, where we know that

$$I_d(x,y) = I_C, \tag{7}$$

by solving it further we can write it as

$$F'(x,y) = \frac{I_a(x,y)}{I_C} = F(x,y) + \frac{\eta(x,y)}{I_c}, \tag{8}$$

where $F'(x,y)$ approximates the reflectance and emittance of the projector because the term $\eta(x,y)/I_c$ is not significant, the acquired patterns: tilt plane and sinusoidal intensity patterns can be normalized, i.e.,

$$I_p \approx \frac{I_a}{F'(x,y)}. \tag{9}$$

In Fig. 3(b) one can see a fringe pattern before correction, where we could observe a nonhomogeneous illumination and the normalized pattern in Fig. 3(c).

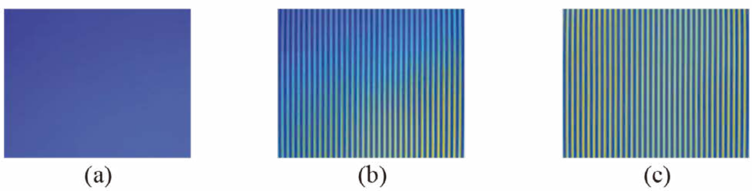

Fig. 3. (a) Captured image with a uniform illuminance on reference plane, sinusoidal intensity pattern; (b) before correction and (c) after normalization.

3.2 Polynomial estimation method

We know that the projector intensity response is determined by power law, that means that if we project intensity ramp in the range from 0 to 255 gray levels in a reference plane. The acquired ramp will be modulated by the power law. We need to estimate the gamma value to correct for the non-linear relationship between projected and acquired gray levels (projected and acquired patents, respectively). An alternative method proposed in the literature is to fit a polynomial of order N to the (normalized) intensity profile, which is obtained from of the linear-wedge grayscale image, previously projected onto the reference plane. The linear-wedge grayscale image to be projected can be described by

$$T(x,y) = R(x), \qquad R(x)\begin{cases}0, & x < 0;\\ x, & 0 \le x \le 255\end{cases}, \tag{10}$$

where the acquired pattern could be a nonlinear intensity map along the tilt axis. All we need to do is the estimation of the coefficient for a polynomial of order N that fit the acquired, nonlinear-wedge grayscale image. For example, third order polynomial,

$$I_{out} = C_0 + C_1 I_{in} + C_2 {I_{in}}^2 + C_3 {I_{in}}^3, \tag{11}$$

with C_0, C_1, C_2, C_3 as the estimated coefficients. For simplicity we will define that the non-linear relationship, between the input and output, which is given by the polynomial, as an operator, $P\{\cdot\}$. Then, we preprocess the input image before inputting it into the DLP by performing the transformation.

When the input into the same projector, the input corrected inverse polynomic produces an output that is close in appearance to the digital image.

$$I'_{in} = 2R(I_{in}) - P\{I_{in}\}, \tag{12}$$

where I_{in} is the ideal intensity and $P\{I_{in}\}$ is the estimated third order polynomial that defines our intensity response model.

3.3 Least squares method

The least squares optimization proposes the estimation of the gamma value as an optimization problem defined by

$$J(\gamma) = \left\|\varphi(x,y)^{1/\hat{\gamma}} - \varphi_p(x,y)\right\|_2^{\;2}, \tag{13}$$

where $\varphi(x,y)^{1/\hat{\gamma}}$ is the unwrapped phase estimated after applying a digital correction in the fringe patterns by certain gamma factor, $\varphi_p(x,y)|_{\varphi^{1/\hat{\gamma}}}$ is the best fitted plane over a region in the unwrapped phase map, and $J(\gamma)$ is the optimization problem solved by a free-derivative for unconstrained minimization problems called the Nelder–Mead simplex method [11], with a range for searching the optimal value.

3.4 Ideal pattern differentiation method

Based on the least squares we propose a new method based on intensity where the estimation of the gamma value is an optimization problem defined by

$$D(\gamma) = \left\|I_n(x) - I(x)^{\hat{\gamma}}\right\|^2, \tag{14}$$

where $I_n(x)$ is a cross-cut of the sinusoidal intensity of acquired pattern when the ideal patterns is projected on reference plane, and $I(x,y)^{\hat{\gamma}}$ is the ideal sinusoidal intensity pattern whose frequency is same to that of the captured pattern, modified with the gamma value, and $D(\gamma)$ is the optimization problem solved by a free-derivative for unconstrained minimization problems called the Nelder–Mead simplex method [11], with a range for searching the optimal value. Once we capture and compensate a sinusoidal pattern, we make a cut in the x axis direction of the pattern retrieved to get a row of data, after compensation we assume that all columns have the same data.

4 Results

In this section, the exposed schemes for gamma calibration are numerically analyzed through computer simulations. However, we also performed a series of experiments with a commercial DLP projector (model PJD7820HD, ViewSonic) with a native spatial resolution of 1920 x 1080 pixels. The images were acquired with an 8-bit single-CCD camera (model DCU 224C, Thorlabs) with a spatial resolution of 1280 x 1024 pixels. The angle in the experiment setup is $\psi \approx 12$ degrees as seen in Fig. 1.

4.1 Simulation

To check the feasibility and validity of the compared methods without the influence of the experimental setup of an FPP system, simulations of 3D measurements of ideal planes distorted by distinct gamma values were carried out. In the first simulation we generated a set of 3 phase shifted fringe patterns for gamma values between 0.2 and 3.9 with increments of one tenth. Each pattern was corrupted with Gaussian noise with different percentages: 2%, 4%, and 6% respectively. We used the root-mean-square error (RMSE):

$$RMSE = \sqrt{\frac{\sum_{n=1}^{N}[\varphi(x,y) - \hat{\varphi}(x,y)]^2}{N}}. \quad (15)$$

Where $\varphi(x, y)$ is the ground truth phase, $\hat{\varphi}(x, y)$ is the estimated phase which is retrieved from the simulated fringe patterns. Fig. 4(a) shows RMSE error in function of gamma value for the three calibration methods under different levels of noise, where one can observe that the polynomial method has worst performance with respect to the least squares and differentiation methods with exceptions around 1 and 1.6. In Fig 4(b) and Fig. 4(c) we observe the RMSE in function of gamma values for the least squares and the differentiation methods, respectively.

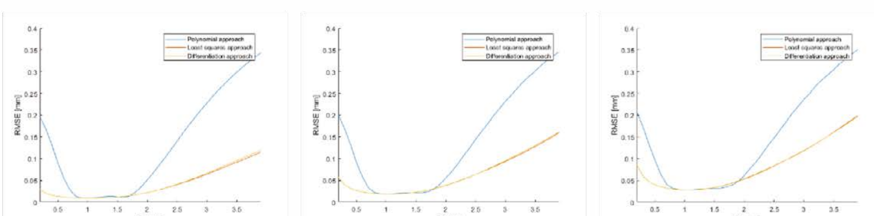

(a) (b) (c)

Fig. 4 Root-mean-square error as a function of gamma value for the methods used for gamma correction: blue, red and yellow lines correspond to: polynomial approach, least squares approach and differentiation approach, respectively. These were evaluated in three different levels of noise: (a) 2%, (b) 4% and (c) 6%.

Table 1. Computer processing time (seconds)

	Noise Level		
Model	2%	4%	6%
Polynomial	0.0092	0.0120	0.0122
Least squares	10.4432	13.8095	13.8255
Differentiation	0.0041	0.0048	0.0050

Table 1 depicts the computer processing time for the data reported on Fig. 4, employing a commercial laptop with an Intel(R) Core (TM) i7-1065G7 CPU and 12GB-DDR4 of RAM, MATLAB R2023b, and Windows 10 as the operating system. We can see in Table 1 that the polynomial and differentiation method have similar computational performances, while the least squares method has higher execution time.

4.2 Experimental results

In this section, we perform a series of experiments to compare performance of previously described three methods to correct the gamma distortion and their effects on retrieved three-dimensional surfaces. As test object was used a resin semi-sphere printed with a precision of 0.05 mm, whose diameter is approximately 60 mm and has a height of 30 mm, the semi-sphere is attached to the plane with double-sided tape with a thickness of approximately 2 mm.

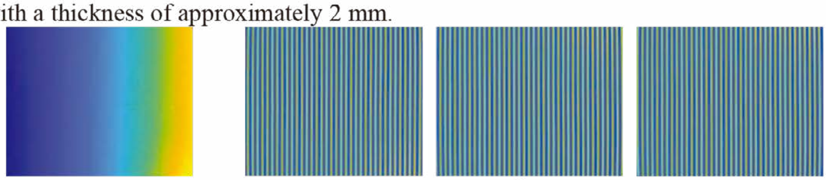

(a) (b)

Fig. 5. Acquired intensity patterns to model the nonlinear intensity response of the projector after the calibration. (a)Tilt plane pattern, (b) 3 phase shift patterns.

At first step, we project and acquire a series of patterns on the reference plane. For the polynomial calibration procedure, a linear-wedge grayscale image was projected sees Fig. 5(a) and three phase shifted patterns, with a pitch of 36 px, see Fig. 5(b).

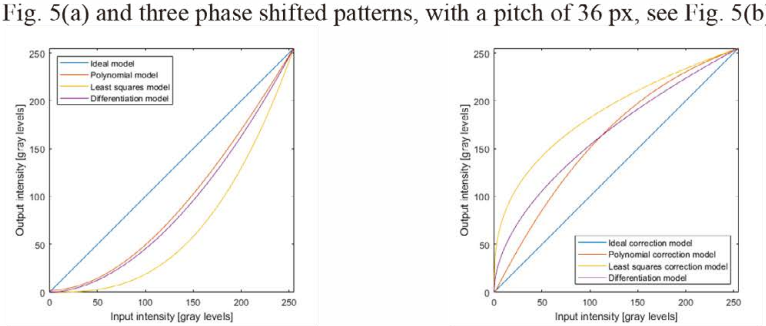

(a) (b)

Fig. 6. Plots the intensity response models acquired by each method reviewed. Being the blue line the ideal model, with the red, yellow and purple line being the polynomial, least squares, and differentiation model respectively. (a) shows the acquired models, while (b) shows their respective correction models.

After the estimation, we get a polynomial function with the following coefficients: -0.3499, 1.3416, 0.0017, 0.0080. and gamma values of 2.7836 and 1.8469 for the least squares and differentiation, respectively, the models can be seen in Fig. 6(a) and the inverse model is shown Fig. 6(b). Next with the estimated correction models we generate fringe patterns to get the wrapped phase with a 36px pitch and shift of $2\pi/3$, and fringe patterns with a pitch of 216px to unwrap the phase based on the double frequency method described in [5], after unwrapping we convert to height through the construction of an empirical model from known surfaces and a linear least squares regression process as described by [12]. After, we compare surface information of an object retrieved with 3 shifted fringe "corrected" patterns, with its respective surface information retrieved with 12 shifted fringe patterns without correction. We do that because as we increase the number of shifted fringe patterns N in a fringe projection profilometer the effects of second and higher order harmonics decrease. 12 shifted fringe patterns should reject the most significant harmonics that distort the phase, giving us a comparison point to review the methods [13].

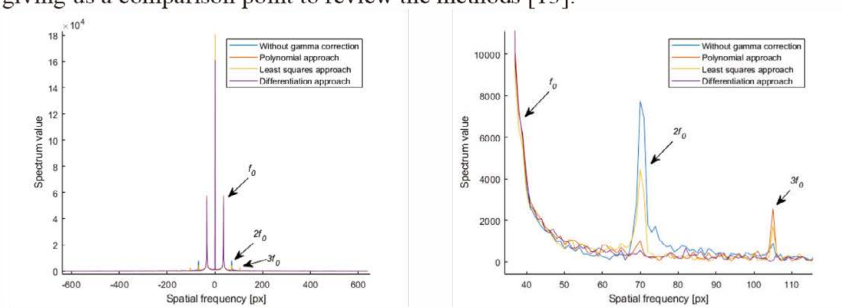

Fig. 7. Plots a frequency domain comparison of gamma corrected pattern with each method reviewed. Being the blue line the 12-steps phase, the red line the 3-steps uncorrected phase, with the red, yellow and purple line being the polynomial, least squares, and differentiation corrected phases respectively. The left figure shows the complete signal, while the right one is a zoom in of the first 3 harmonics.

With that we proceed to recover 3D measurement of the object as a final test. In simulations, the least squares and differentiation methods have similar performances even though the estimated values have a difference of almost 1; this deviation is seen in Fig. 6 and it is because of the mathematical model of the least squares is sensitive to small deviations in the estimated value and despite that, we can observe that both methods correct partially the gamma distortion as we can see in Fig. 7, Fig. 8, and Fig. 9. In Fig. 7 we can observe the amplitude of the harmonics, in the Fourier domain, of a fringe pattern corrected by each method. In Fig. 9, we can see that the polynomial method and differentiation method have better results. However, In Fig. 7 conclude the method that best cancels the harmonics is the differentiation one. Also, in experimental results, Fig. 8, This is observed better in the horizontal cut of the phase in Fig. 9 and in Fig. 8 we confirm that the methods that best cancel the ripple in the object height profile are the methods, this ripple is due to the second harmonic. Assuming that the ideal reconstruction is the one obtained by the 12-step method, we estimate the rms value for each method: RMSE for the uncorrected 3-step algorithm was 0.4895 mm. While RMSE values for the polynomial method, least squares method and differentiation method were 0.21 mm, 0.32mm, and 0.22mm, respectively.

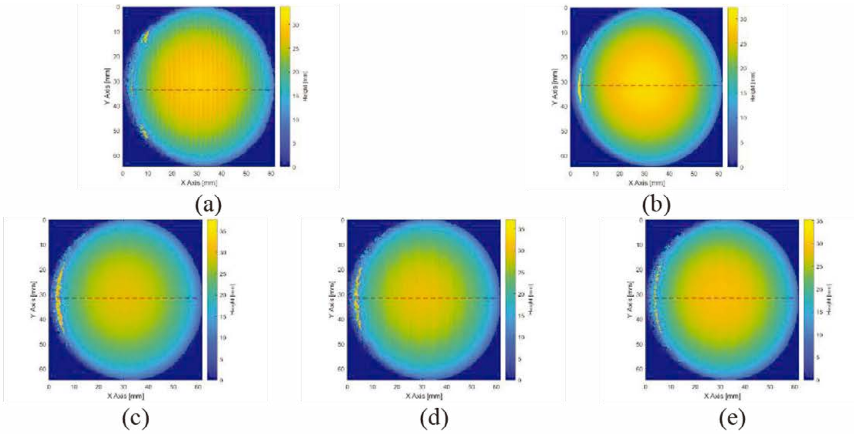

Fig. 8. Comparison of a horizontal of the phase of an object by each reviewed method. Being the red line a horizontal cut. (a) Shows the 3 steps phase without corrections and (b) the 12 steps phase, while (c) shows a 3 steps phase by the polynomial approach, (d) a 3 steps phase by the least squares approach, and (e) a 3 steps phase by the differentiation method.

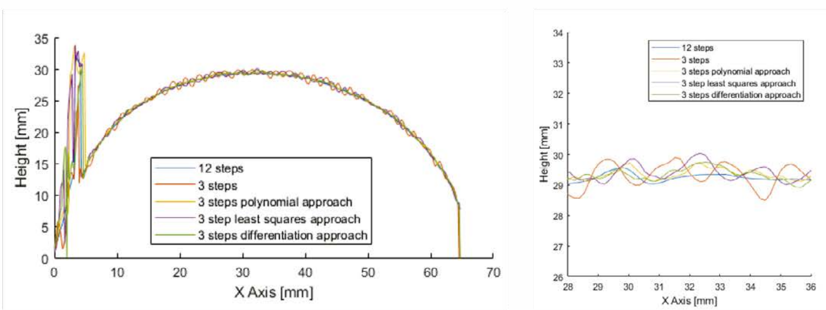

Fig. 9. Comparison of a horizontal cut of the phase of an object by each reviewed method. Being the blue line the 12-steps phase, the red line the 3-steps uncorrected phase, with the red, yellow and purple line being the polynomial, least squares, and differentiation corrected phases respectively. The left figure shows the complete signal, while the right one is a zoom in.

5 Conclusions

In this work, we present a new scheme to estimate the gamma of a projection system proposed for reconstructing and measuring 3D surfaces. The estimation is performed as an optimization problem, where the objective function is the difference between the sinusoidal intensity of acquired pattern and its ideal sinusoidal intensity pattern (gamma modified) whose spatial frequency and phase are the same as that of the acquired pattern.

Also, we compare its performance with two other calibration methods, the least squares, and the polynomial method. In simulations, we found that the proposed method and the least squares have similar gamma-correcting performances with lower RMSE over a wider range of gamma values in contrast with the polynomial the latter being slightly better around a gamma value of 1.6.

We implemented and tested these calibration methods on a fringe projection profilometer. Experimentally, the proposed method, the least squares method and polynomial method reduced the RMSE by a factor of 2.15, 1.52, and 2.32, respectively. Where the proposed method and the polynomial method have similar performances, but unlike the polynomial, it is not necessary to acquire a tilt plane to estimate the nonlinear intensity response of the projector. Therefore, our algorithm requires only a sinusoidal pattern and can be useful in dynamic applications, where having high processing speed is essential.

References

1. R. P. Johnson, Qingping Yang and C. Butler, "Dynamic error characteristics of touch trigger probes fitted to coordinate measuring machines," in *IEEE Transactions on Instrumentation and Measurement*, vol. 47, no. 5, pp. 1168-1172 (1998).
2. Song Zhang, Recent progresses on real-time 3D shape measurement using digital fringe projection techniques, Optics and Lasers in Engineering, Volume 48, Issue 2, Pages 149-158, ISSN 0143-8166 (2010).
3. J. Geng, "Structured-light 3D surface imaging: a tutorial," Adv. Opt. Photon. 3, 128-160 (2011).
4. M. Servin, J. A. Quiroga, and M. Padilla, Fringe Pattern Analysis for Optical Metrology: Theory, Algorithms, and Applications (Wiley, 2014).
5. Servín, Manuel & Padilla, Moises & González, Christhian & Garnica, Guillermo. Temporal phase-unwrapping of static surfaces with 2-sensitivity fringe-patterns. Optics Express (2015).
6. Chao Zuo, Lei Huang, Minliang Zhang, Qian Chen, Anand Asundi, Temporal phase unwrapping algorithms for fringe projection profilometry: A comparative review, Optics and Lasers in Engineering, Volume 85, 2016, Pages 84-103, ISSN 0143-8166 (2016).
7. Zhaoyang Wang, Dung A. Nguyen, John C. Barnes, Some practical considerations in fringe projection profilometry, Optics and Lasers in Engineering, Volume 48, Issue 2, Pages 218-225, ISSN 0143-8166 (2010).
8. Jun Yao, Hong Miao, Jubing Chen, Calibration of fringe projection system for surface profile measurement, Optical Engineering, Vol. 56, Issue 3, 034109 (2017).
9. P.S.Huang, C.Zhang, and F.P.Chiang, "High-speed 3-D shape measurement based on digital fringe projection," Opt. Eng. 42, 163–168 (2003).
10. A. Muñoz, J. Flores, G. Parra-Escamilla, L. Morales, S. Ordones, and M. Servin, "Least-squares gamma estimation in fringe projection profilometry," Appl. Opt. 60, 1137-1142 (2021).
11. J. A. Nelder and R. Mead, "A simplex method for function minimization," Comput. J. 7, 308–313(1965).
12. Jia, Peirong & Kofman, Jonathan & English, Chad. Comparison of linear and nonlinear calibration methods for phase-measuring profilometry. Optical Engineering - OPT ENG. 46 (2007).
13. Z. Li and Y. Li, "Gamma-distorted fringe image modeling and accurate gamma correction for fast phase measuring profilometry," Opt. Lett. 36, 154-156 (2011).